CHIMIA **2006**, *60*, No. 1/2

Chimia 60 (2006) 70–75

ISSN 0009–4293

A Thorough Training in *Modern Drug Design*

Angelo Vedani*, Oliver Schwardt, Said Rabbani, and Beat Ernst

Abstract: The laboratory class *Modern Drug Design* at the Department of Pharmacy of the University of Basel offers the students a thorough training in modern drug design. First, antagonists for the Bradykinin B_2 receptor are designed using state-of-the-art modelling techniques, followed by solid-phase synthesis of the most potent candidates identified *in silico*. Thereafter, their activity is determined by a fluorometric assay. By communicating the results to the next class of students, a feedback loop is completed, thereby allowing the design strategy to be improved.

Keywords: Bradykinin · Bradykinin receptor · Education · Modern drug design

Introduction

While the laboratory section *Modern Drug Design* offers the students hands-on experience in design, synthesis and assay of potential drug candidates, a number of classes provide the theoretical background for successful application of the concepts. At the Department of Pharmacy of the University of Basel such classes include *Mechanisms of Molecular Action*, *Introduction into Molecular Modeling*, *Bioinorganic Chemistry,* and a *Drug Discovery Seminar series*. In addition, virtual training in selected technologies (*e.g.* SDS page chromatography) is offered as part of the video-based interactive learning tool *ViLab* (see *http://www.pharmasquare.org*).

Bradykinin, a nonapeptide (Arg–Pro–Pro–Gly–Phe–Ser–Pro–Phe–Arg) released from plasma globulins known as kininogens in a variety of inflammatory conditions, is a potent vasodilatator, which increases vascular permeability, stimulates pain receptors, and causes contraction of a variety of extravascular smooth muscles [1][2]. Consequently, it has raised substantial interest within the pharmaceutical community. Angiotensin-converting enzyme (ACE), an endopeptidase, converts angiotensin I to angiotensin II but also accepts Bradykinin as a substrate, thereby reducing the vasodilative effect exerted by the latter. Molecules that inhibit ACE are used as anti-hypertensive drugs [3]. In pathological situations such as oedema, septic shock and inflammatory reactions, Bradykinin is not beneficial, and Bradykinin antagonists are of interest [4]. Up to now, two Bradykinin receptors have been identified [5]: the B_1-type receptor which is predominantly expressed in the muscle tissue of smaller blood vessels and the B_2-type receptor which is found in different tissues. The binding of Bradykinin to the B_2 receptor (K_d = 1–12 nM) leads to the activation of a membrane phospolipase C, which hydrolyses phosphatidylinosite-4,5-diphosphate (PIP_2) to myoinosite-1,4,5-triphosphate (IP_3) and diacylglycerol (DAG). DAG remains in the inner layer of the plasma membrane whereas IP_3 opens calcium channels in the endoplasmic reticulum (ER), releasing free Ca^{2+} into the cytosol. The rapid increase in the cytosolic Ca^{2+} concentration regulates several cellular reactions.

*Correspondence: Prof. Dr. A. Vedani
Institute of Molecular Pharmacy
Department of Pharmaceutical Sciences
Pharmacenter
University of Basel
Klingelbergstrasse 50
CH-4056 Basel
Tel.: +41 61 267 1503
E-Mail: angelo.vedani@unibas.ch

Part I: Modeling the Bradykinin B_2 Receptor

As no experimental structure is available for the Bradykinin B_2 receptor, we generated and validated a quasi-atomistic receptor surrogate (a binding-site model) using the *Quasar* technology, a 6D-QSAR tool [6][7]. *Quasar* generates a family of quasi-atomistic receptor models that are optimized by means of a genetic algorithm. The hypothetical receptor site is characterized by a three-dimensional surface that surrounds the ligand molecules at the van der Waals distance and which is populated with atomistic properties mapped onto it. The topology of this surface mimics the 3D shape of the binding site; the mapped properties represent other information of interest, such as hydrophobicity, electrostatic potential, and hydrogen-bonding propensity (Fig. 1).

The fourth dimension (4D-QSAR) in *Quasar* refers to the possibility of representing each ligand molecule as an ensemble of conformations, orientations, and protonation states, thereby reducing the bias in identifying the bioactive conformation and orientation. Within this ensemble, the contribution of an individual entity to the total energy is determined by a normalized Boltzmann weight. Because the manifestation and magnitude of the induced fit may vary for different molecules binding to a target protein, *Quasar* allows for the simultaneous evaluation of up to six different induced-fit protocols (5D-QSAR). The most recent extension of the *Quasar* concept to six dimensions (6D-QSAR) allows for the simultaneous consideration of different solvation models [7]. This can be achieved explicitly by mapping parts of the surface area with solvent properties (position and size are optimized by the genetic algorithm), or implicitly. In *Quasar*, the binding energy is calculated as follows:

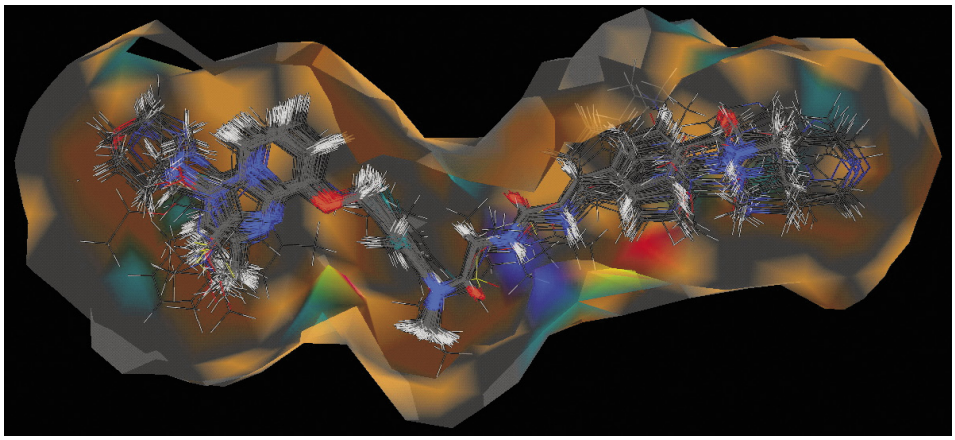

Fig. 1. Quasi-atomistic model of the Bradykinin B_2 receptor as generated with *Quasar* (*cf.* text). Color coding: red = positively charged salt bridge, blue = negatively charged salt bridge, green = H-bond donor, yellow = H-bond acceptor, grey = neutral hydrophobic, saddle brown = positively charged hydrophobic, chocolate brown = negatively charged hydrophobic. The pharmacophore hypothesis (3D alignment of the ligand molecules) was generated using the *Symposar* technology.

$$E_{binding,\ ligand} = E_{ligand\text{-}receptor} - T\Delta S_{binding} - E_{solvation} - \Delta E_{internal\ strain} - E_{induced\ fit}$$

Based on data published by Fujisawa Pharmaceuticals Ltd. (see *e.g.* [8]), we selected a set of 153 Bradykinin B_2 antagonists ranging from 10 mM to 0.13 nM in their IC_{50} values. The three-dimensional structure of all molecules was generated and optimized in aqueous solution using the AMBER force field as implemented in the *MacroModel* software [9]. Next, a conformational search was conducted for selected ligand molecules to assess their conformational flexibility. The pharmacophore hypothesis (3D alignment) was then generated using the *Symposar* technology [10]. Of the 153 ligand molecules 118 were composed into the training set, the remaining 35 defined the test set.

The simulation on the Bradykinin B_2 receptor was based on a family of 200 models, and was evolved for 16,000 crossovers, corresponding to 80 generations. It converged at a cross-validated r^2 of 0.798 and yielded a predictive r^2 of 0.793. The maximal deviation from the experiment corresponds to a factor 12.9 in IC_{50} for the ligands of the training set and to a factor 12.9 for the ligands of the test set [11]. The model is shown in Fig. 1, the correlation of the predicted and experimental IC_{50} values is shown in Fig. 2.

Next, the students generated new potential Bradykinin B_2 antagonists using the functional group analysis tool implemented in *Quasar* (it breaks the contribution of the free energy of ligand binding down to individual functional groups, allowing the identification and improvement of 'molecular weaknesses'). Starting off from Fujisawa's most potent compounds [8], they aimed to improve the ligand–receptor interaction, but simultaneously keeping the cost of ligand desolvation at a modest rate (by exchanging polar/apolar groups that give rise to only weak interactions with the receptor surrogate), as well as reducing entropic effects (by including further rigid elements such as double bonds and rings). Out of a total of 120 suggested new compounds, some twenty were calculated to bind in the low nanomolar range – five were calculated to bind with an IC_{50} <1.0 nM, the best at 0.065 nM (Fig. 3).

Of course, attention was also paid to synthetic accessibility and metabolic stability as these factors are known to be crucial for successful drug design. As the follow-up laboratory section includes the synthe-

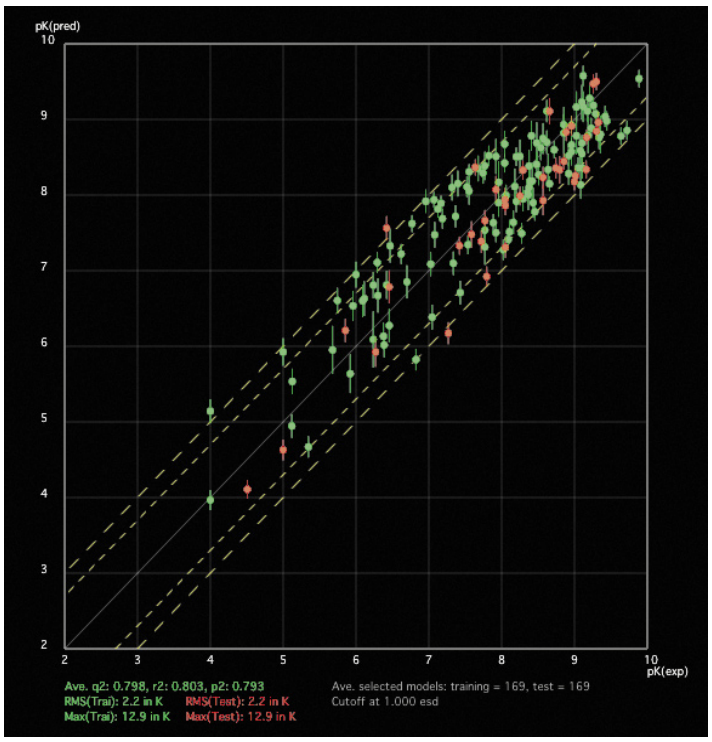

Fig. 2. Comparison of experimental and calculated IC_{50} values. Green dots represent ligands of the training set, red dots those of the test set. Dashed lines are drawn at factors 5.0 and 10.0 off the experiment.

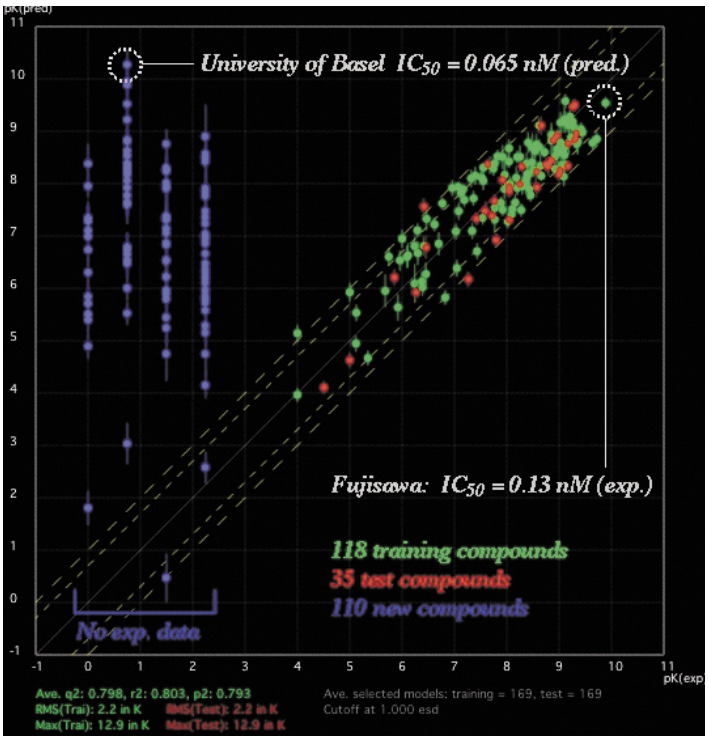

Fig. 3. Comparison of experimental and calculated IC_{50} values. Green (training set) and red dots (test set) represent the Fujisawa data set (*cf.* Fig. 2), the blue dots those designed by the 2004/5 student class. For the latter, no experimental data is yet available as they still await chemical synthesis.

sis of the predicted compounds on solid phase (*cf.* part II below), the students also suggested novel peptidic inhibitors starting from Bradykinin (Arg-Pro-Pro-Gly-Phe-Ser-Pro-Phe-Arg and HOE-140 (Arg-Arg-Pro-Hyp-Gly-Thi-Ser-Tic-Oic-Arg). The same procedure was used as for the peptidomimetics (model building and validation), and a total of 21 new peptidic compounds were designed, the best of which was predicted to bind with an IC_{50} of 0.023 nM. The feedback received from the biological assays of the first four classes (2004/5; see the Table below) will allow us to improve this year's design cycle.

Part II: Solid-phase Synthesis of Bradykinin Analogs

In the second section of the practical course, the students have the possibility to synthesize the peptidic Bradykinin antagonists they have designed in the molecular modeling section using solid-phase peptide synthesis.

The chemical synthesis of peptides [12] can be carried out either in solution or on solid phase. In solution, isolation and purification of the intermediate products is required after each coupling step. This repetitive procedure is both time and material consuming. In contrast, in solid-phase synthesis all intermediates remain bound to the solid support, and only the final product needs to be purified (Scheme 1). The first protected amino acid is anchored to the insoluble polymer support by means of a flexible, selectively cleavable linker. The peptide chain is elongated in the C- to N-direction through repetitive cycles of N-terminus deprotection and coupling. All soluble reagents are removed by washing after each step. Throughout the synthesis any functional groups in amino acid side-chains must be permanently protected to withstand the coupling conditions. At the end of the synthesis, the side-chain protecting groups are removed together with the detachment of the peptide from the polymer support in one step.

In our laboratory course, *SynPhase*™ lanterns (Mimotopes Pty. Ltd., Melbourne, Australia) equipped with the acid-labile Rink-amide linker are used. They consist of a polystyrene (PS) grafted surface that has similar performance characteristics to conventional polystyrene resins (Fig. 4).

The peptides are synthesized according to the Fmoc-strategy [13]. In this strategy, the N-α protecting group is the mild base-sensitive Fmoc-group, whereas all functionalities in amino acid side-chains are orthogonally protected by base-stable and acid-labile groups like Boc, trityl and *t*-butyl. Cleavage of the Fmoc group is done with a 20% solution of piperidine in N,N-

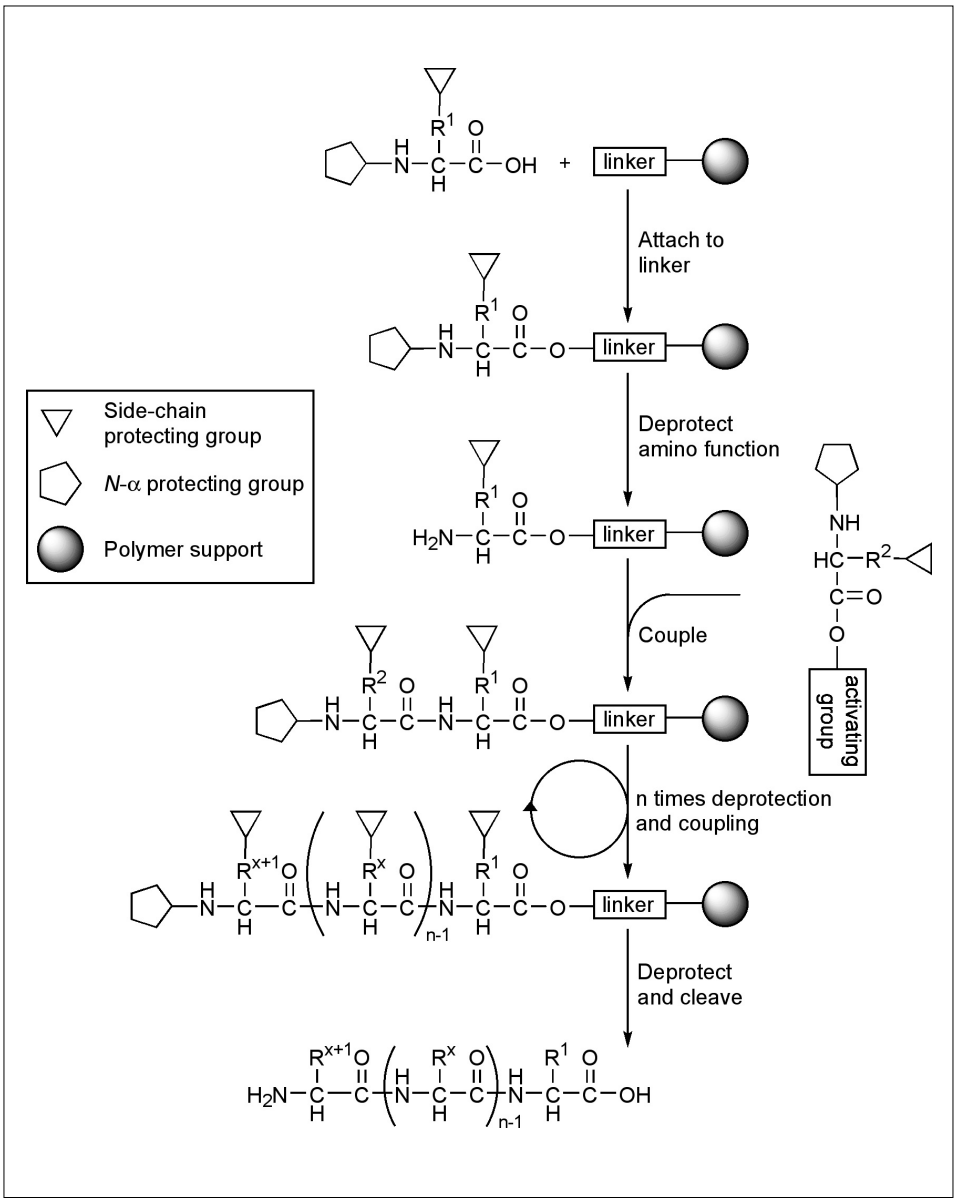

Scheme 1. Schematic diagram of solid phase peptide synthesis

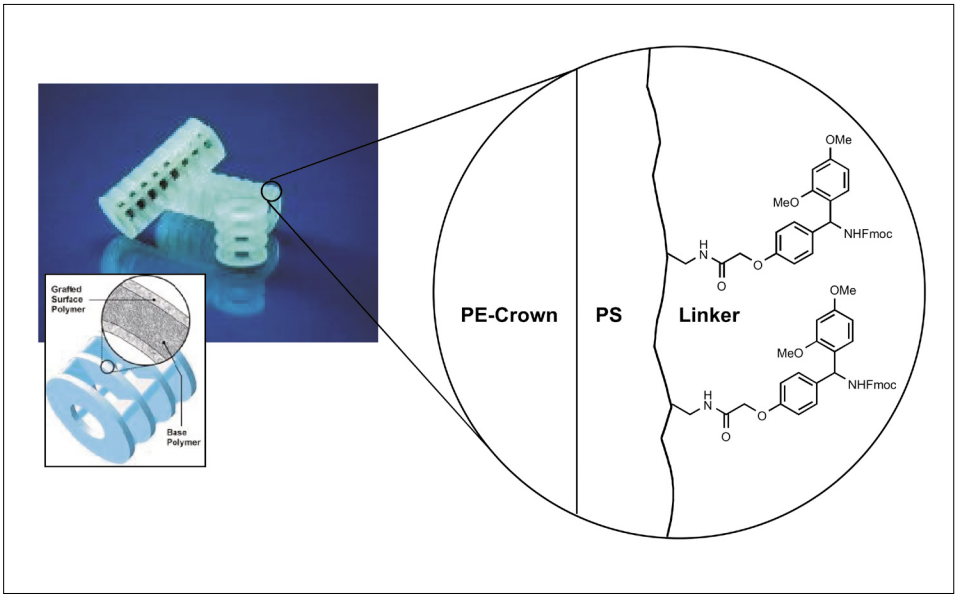

Fig. 4. SynPhase™ lanterns equipped with *Rink* amide linkers

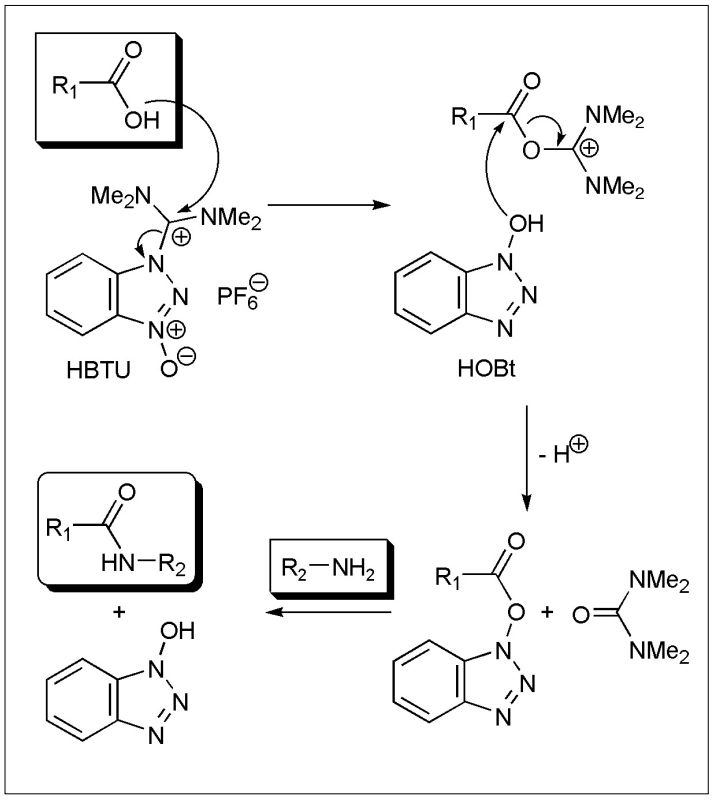

Scheme 2. Coupling mechanism using HBTU and HOBt

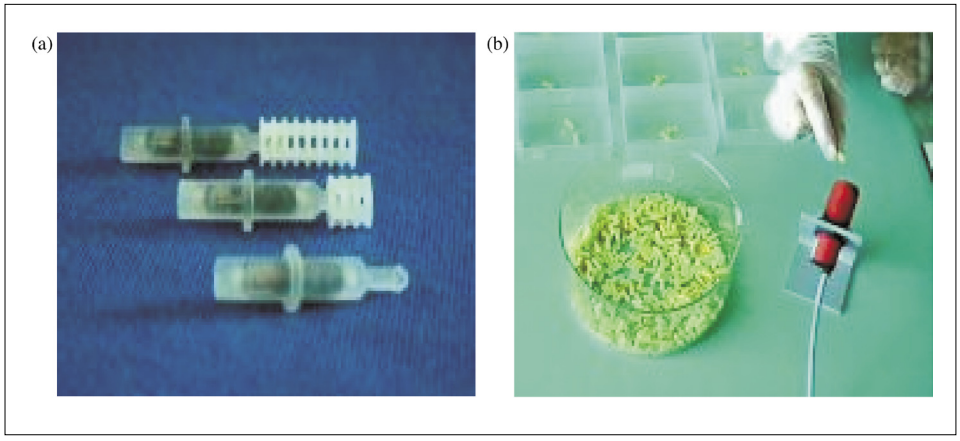

Fig. 5. a) SynPhase™ lanterns with RF tags; b) TranSort™ antenna for the identification of RF tags

dimethylformamide (DMF). The coupling steps are carried out according to standard procedures [14] with 2-(1*H*-benzotriazole-1-yl)-1,1,3,3-tetramethyluronium hexafluorophosphate (HBTU)/N-hydroxybenzotriazole (HOBt) and diisopropylethylamine (DIPEA) as coupling reagents (Scheme 2). Trifluoracetic acid (TFA) is used for the final cleavage of the acid-labile linker group and side-chain deprotection.

For training purposes, the students first synthesize a 3×3×3-library of 27 tripeptides using combinatorial (parallel) synthesis. The identification of the peptides is done with radiofrequency (RF) tagging (Fig. 5). Some of the tripeptides are then cleaved from the solid support and analyzed for purity by HPLC.

In the second part of the laboratory course, the students synthesize the nonapeptides they have designed in the molecular modeling section. Starting from the pre-formed tetrameric peptide Fmoc-Ser-Pro-Phe-Arg-Rink, the nonapeptides are reached by five cycles of N-deprotection and coupling. Natural as well as non-natural amino acid building blocks can be used. The nonapeptides are then cleaved from the solid phase and analyzed by HPLC and mass spectrometry (MS). Finally, the crude peptides are purified by preparative LC-MS using a reversed-phase column C_{18} with acetonitrile/water mixtures (for an example, see Fig. 6). Usually 5–10 mg of pure (>90% HPLC purity) nonapeptide are obtained after a final lyophilization from water. The Bradykinin analogs are then tested for their Ca^{2+} mobilizing effect in PC-12 cells.

The synthetic work is accompanied by intensive HPLC training; an integrative part of this laboratory course. The students get several unknown mixtures of 2–4 substances, usually drugs. For these samples, optimal separation methods have to be worked out (mobile phase, gradient, detection wavelength). The students then have to analyze the chromatograms and state the reasons why various compounds have different retention times by examining the physicochemical properties of the former (*e.g.* alkyl groups *vs*. charged moieties).

Part III: Fluorometric Assay

The third part of the practical course is divided into two sections: The first section provides training in protein extraction and analysis methods. The techniques covered are SDS-PAGE and Western blot analysis of the Bradykinin receptor. Virtual laboratory modules (*ViLabs*, see article by C. Weber *et al*. [15] in this issue) support the students in both understanding the scientific background and learning the corresponding laboratory techniques. In this section, the Bradykinin antagonists – that were designed *in silico* and synthesized on solid phase – are tested for their calcium mobilizing effect. The change in Ca^{2+} concentration is monitored with a fluorometric assay using PC12 cells (Fig. 7) and the fluorescence indicator Fura-2 (Fig. 8).

The Ca^{2+} fluorescence indicator Fura-2 [16] has become the dye of choice used for detecting changes in intracellular calcium concentrations. The acetoxymethyl (AM) ester form of Fura-2 can passively diffuse across cell membranes. Once inside the cell, the esters are cleaved by intracellular esterases to yield the cell-impermeant fluorescent indicator. Upon binding to Ca^{2+} (K_d = 135 nM), Fura-2 exhibits an absorption shift that can be observed at excitation wavelengths of 380 nm (free Fura-2) and 340 nm (Ca^{2+}-bound Fura-2), while monitoring the emission at 515 nm. The intracellular calcium concentration can be determined according to the equation derived by Grynkiewicz *et al.* [17].

$$[Ca^{2+}]_i = K_d \cdot (F_{min}/F_{max}) \cdot (R-R_{min}) / (R_{max}-R)$$

K_d is the dissociation constant of the Ca^{2+}-Fura-2 complex, F_{min} and F_{max} are the fluorescence intensities obtained from Ca^{2+}-free Fura-2 sample and Ca^{2+}-bound Fura-2 sample, respectively, R is the fluorescence intensity ratio obtained with ex-

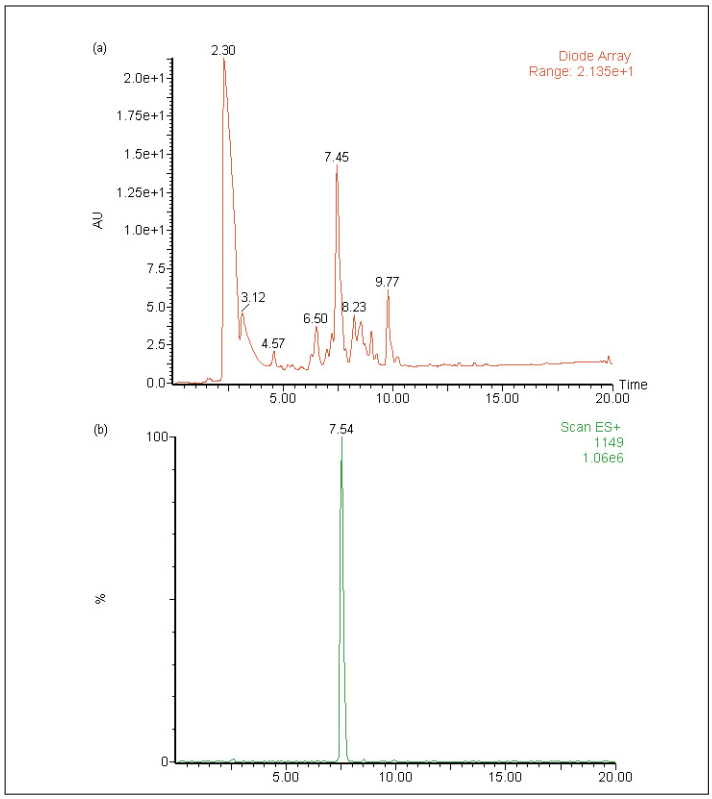

Fig. 6. LC-MS purification of nonapeptide Arg-Phe-Pro-Gly-Trp-Ser-Pro-Phe-Arg (preparative C18-column Waters SunfireTM, 5 mm, 19x150 mm; water/acetonitrile + 0.2% formic acid, flow rate 15 mL/min), (a) UV chromatogram (210-400 nm); (b) collected fraction (ES, positive mode, $[M+H]^+$ 1149)

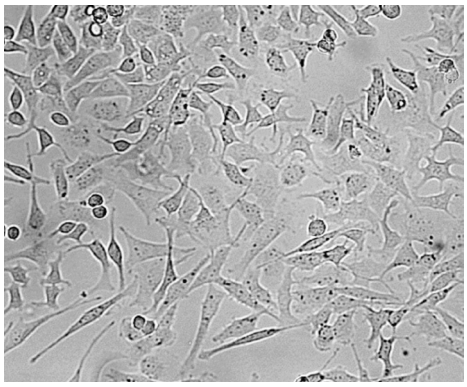

Fig. 7. Rat PC12, pheochromocytoma cells: a clonal cell line frequently used to investigate the cytosolic change in calcium concentration in response to various molecules. The micrograph shows differentiated cells (20X).

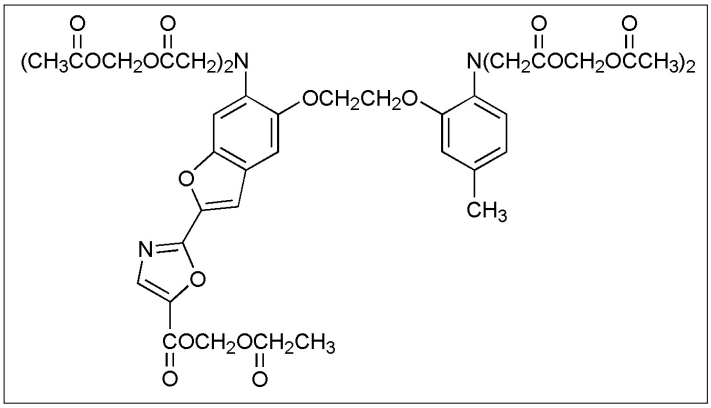

Fig. 8. Fura-2AM, a fluorescent Ca^{2+}-sensitive dye. After diffusion across the cell membrane, Fura-2AM is hydrolyzed to active Fura-2 by cytosolic esterases. When Fura-2 binds to Ca^{2+}, the effective excitation wavelength shifts from 380 to 340 nm. This property is used to measure local Ca^{2+} concentration changes within cells.

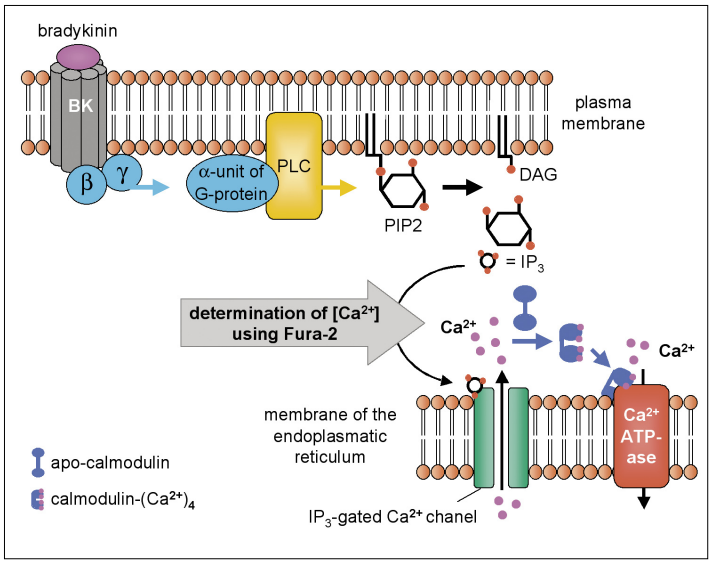

Fig. 9. The binding of Bradykinin to G protein-coupled Bradykinin receptor (BK) leads to the activation of a membrane phospholipase C (PLC). PLC hydrolyses phosphatidylinosite-4,5-diphosphate (PIP_2) to myoinosite-1,4,5-triphosphate (IP_3) and diacylglycerol (DAG). DAG remains in the plasma membrane, whereas IP_3 opens IP_3-gated calcium channels in the endoplasmic reticulum, releasing Ca^{2+} into the cytosol. The $[Ca^{2+}]$ is measured by fluorescence at excitation wavelength of 340 nm caused by the chelation of Ca^{2+} by Fura-2.

citation at 340 and 380 nm ($R = F_{340}/F_{380}$), R_{min} and R_{max} are the F_{340}/F_{380} ratios of the calcium-free and calcium-saturated Fura-2 samples, respectively.

Rat PC12 (pheochromocytoma cells) is a clonal cell line frequently used as a nerve cell model [18]. Differentiated cells exhibit a variety of properties similar to neurons, including the overall phenotype and the expression of membrane receptors. In addition, PC12 cells are frequently used to investigate the cytosolic change in calcium concentration in response to various molecules. The presence of the Bradykinin receptor makes these cells very suitable for this assay [19]. The cellular response to Bradykinin and its derivatives can be monitored by fluorometry. The principle of the fluorometric assay is schematically depicted in Fig. 9. The correlation of Ca^{2+} and Bradykinin antagonist concentrations permits the qualitative and quantitative evaluation of the nonapeptide effect.

Results and Conclusions

A summary of the modeled, synthesized, and assayed nonapeptides is given in the Table. Out of the twenty-one modeled compounds, fourteen were successfully synthesized along with four candidates not previously modeled. Fifteen out of the latter compounds could be assayed for activity. While a fair overall agreement can be observed, some of the *in silico* predictions could not be confirmed *in vitro*. This can be attributed to two principle sources of error: (i) the model for the peptidic

Table. Summary of the designed, synthetized, and assayed peptidic Bradykinin B_2 inhibitors. Non-standard amino acids include hydroxyproline (Hyp), isonipecotic acid (Ina), and cylcohexylalanine (Cal). The four C-terminal amino-acid residues (^+H_3N-X–X–X–X–Ser–Pro–Phe–Arg-COO^-) were identical for all peptides (*cf.* synthesis section). Differences with respect to Bradykinin are highlighted in bold.

Code	Compound	IC_{50} calc.	Synthesis	Bioassay
BRK	Arg–Pro–Pro–Gly–Phe–Ser–Pro–Phe–Arg	2.7×10^{-10}	n/a	Reference
P32	Arg–**Ile**–Pro–Gly–Phe–Ser–Pro–Phe–Arg	2.3×10^{-11}	✓	–
P21	**His**–**Hyp**–Pro–Gly–**Ile**–Ser–Pro–Phe–Arg	3.2×10^{-10}	✓	weak agonist
P25	**His**–**Leu**–Pro–Gly–**His**–Ser–Pro–Phe–Arg	6.8×10^{-10}	✓	–
P43	Arg–**Ina**–Pro–Gly–Phe–Ser–Pro–Phe–Arg	1.2×10^{-9}	✓	weak agonist
P41	Arg–Pro–Pro–Gly–**Cal**–Ser–Pro–Phe–Arg	1.3×10^{-9}	–	
P44	Arg–**Ina**–Pro–Gly–**Cal**–Ser–Pro–Phe–Arg	2.2×10^{-9}	–	
P33	Arg–**Leu**–**Hyp**–Gly–Phe–Ser–Pro–Phe–Arg	3.2×10^{-9}	✓	agonist
P24	**Lys**–**Leu**–Pro–Gly–**His**–Ser–Pro–Phe–Arg	8.3×10^{-9}	✓	as Bradykinin
P22	**His**–Pro–Pro–Gly–**Ile**–Ser–Pro–Phe–Arg	1.7×10^{-8}	–	
P25	**His**–**Leu**–Pro–Gly–**His**–Ser–Pro–Phe–Arg	2.4×10^{-8}	–	
P23	**Lys**–**Hyp**–Pro–Gly–**His**–Ser–Pro–Phe–Arg	3.4×10^{-8}	✓	as Bradykinin
P14	Arg–**Val**–Pro–Gly–**Tyr**–Ser–Pro–Phe–Arg	7.2×10^{-8}	–	
P15	**Lys**–Pro–Pro–Gly–**Tyr**–Ser–Pro–Phe–Arg	1.9×10^{-7}	–	
P45	Arg–Pro–**Ina**–Gly–**Cal**–Ser–Pro–Phe–Arg	3.5×10^{-7}	–	
P34	Arg–Pro–**Hyp**–Gly–Phe–Ser–Pro–Phe–Arg	5.2×10^{-7}	✓	antagonist
P42	Arg–Pro–**Ina**–Gly–Phe–Ser–Pro–Phe–Arg	1.7×10^{-6}	✓	weak agonist
P12	**Gln**–**Gly**–Pro–Gly–Phe–Ser–Pro–Phe–Arg	3.0×10^{-6}	✓	weak agonist
P35	Arg–**Leu**–Pro–Gly–Phe–Ser–Pro–Phe–Arg	3.9×10^{-5}	✓	weak antagonist
P11	Arg–**Phe**–Pro–Gly–**Trp**–Ser–Pro–Phe–Arg	3.4×10^{-4}	✓	agonist
P31	Arg–**Leu**–**Hyp**–Gly–Phe–Ser–Pro–Phe–Arg	3.5×10^{-3}	✓	agonist
P13	**Lys**–Pro–Pro–Gly–**Trp**–Ser–Pro–Phe–Arg	$>10^{-2}$	✓	weak agonist
X41	**Cal–Gly–Pro–Pro–Arg**–Ser–Pro–Phe–Arg	–	✓	weak agonist
X44	**Cal–Gly–Pro–Ina–Arg**–Ser–Pro–Phe–Arg	–	✓	weak antagonist
X21	**Ile–Gly–Pro–Pro–His**–Ser–Pro–Phe–Arg	–	✓	–
X45	**Cal–Gly–Ina–Pro–Arg**–Ser–Pro–Phe–Arg	–	✓	antagonist

compounds could only be validated on a small set of data (25 quite similar peptides compared to the 153 diverse pepdidomimetics, *cf.* above), and (ii) to the difficulty in producing clean data from a single biological assay. Due to problems associated with the purification protocol, a total of seven peptides could not be successfully synthesized. Nonetheless, the results can be considered a great success for having imparted the students a realistic scenario of modern drug design.

Received: January 16, 2006

[1] A. Dray, M. Perkins, *Trends Neurosci.* **1993**, *16*, 99–104.

[2] P.D. Cherry, R.F. Furchgott, J.V. Zawadzki, D. Jothianandan, *Proc. Natl. Acad. Sci. USA* **1982**, *79*, 2106–2110.

[3] a) W.W. Brooks, O.H. Bing, K.G. Robinson, M.T. Slawsky, D.M. Chaletsky, C.H. Conrad, *Circulation* **1997**, *96*, 4002–4010; b) H. Peng, O. A. Carretero, N. Vuljaj, T.D. Liao, A. Motivala, E. L. Peterson, N.E. Rhaleb, *Circulation* **2005**, *112*, 2436–2445.

[4] J.R. Cockcroft, P.J. Chowienczyk, S.E. Brett, N. Bender, J.M. Ritter, *Br. J. Clin. Pharmacol*. **1994**, *38*, 317–322.

[5] D. Rigoli, J. Barabé, *Pharmacol. Rev.* **1980**, *32*, 1–46.

[6] A. Vedani, M. Dobler, M.A. Lill, *J. Med. Chem.* **2002**, *45*, 2139–2149.

[7] a) A. Vedani, M. Dobler, M.A. Lill, *J. Med. Chem.* **2005**, *48*, 3700–3703 b) A. Vedani, M. Dobler, M.A. Lill, *J. Med. Chem.* **2005**, *48*, 1515–1527.

[8] Y. Sawada, H. Kayakiri, Y. Abe, T. Mizutani, N. Inamura, M. Asano, I. Aramori, C. Hatori, T. Oku, H. Tanaka, *J. Med. Chem*. **2004**, *47*, 2667–2677.

[9] F. Mohamadi, N.G.J. Richards, W.C. Guida, R. Liskamp, M. Lipton, C. Caufield, G. Chang, T. Hendrickson, W.C. Still, *J. Comput. Chem.* **1990**, *11*, 440–467.

[10] M.A. Lill, M. Dobler, A. Vedani, *J. Chem. Inf. Model.*, in preparation.

[11] *http://www.modeling.unibas.ch/UB_BB2.html*

[12] a) M.F. Songster, G. Barany, *Methods Enzymol.* **1997**, *289*, 126–174; b) K.H. Altmann, M. Mutter, *Chemie in unserer Zeit* **1993**, *27*, 274–286.

[13] a) 'Fmoc Solid Phase Peptide Synthesis: A Practical Approach', W.C. Chan, P.D. White, Eds., Oxford University Press, **2000**, pp 1–74; b) B. Fields, R.L. Nobel, *Int. J. Peptide Protein Res.* **1990**, *35*, 161–214.

[14] R. Breinbauer, I.R. Vetter, H. Waldmann, *Angew. Chem*. **2002**, *114*, 3002–3015.

[15] C. Weber, A. Vögtli, A. Ensner, A.-B. Utelli, *Chimia* **2006**, *60*, 66–69.

[16] J.P. Kao, *Methods Cell Biol.* **1994**, *40*, 155–181.

[17] G. Grynkiewicz, M. Poenie, R.Y. Tsien, *J. Biol. Chem.* **1985**, *260*, 3440–3450.

[18] L.A Greene, A.S. Tischler, *Proc. Natl. Acad. Sci. USA* **1976**, *73*, 2424–2428.

[19] J. Nardone, C. Geraldi, L. Rimawi, L. Song, P.G. Hogani, *Proc. Natl. Acad. Sci. USA* **1994**, *91*, 4412–4416.